JACS
JOURNAL OF THE AMERICAN CHEMICAL SOCIETY

Article

pubs.acs.org/JACS

Light-Induced Charge Separation in Densely Packed Donor–Acceptor Coordination Cages

Marina Frank,[†] Jennifer Ahrens,[‡] Isabel Bejenke,[†] Marcel Krick,[†] Dirk Schwarzer,[‡] and Guido H. Clever*[,†,§]

[†]Institute for Inorganic Chemistry, Georg-August University Göttingen, Tammannstraße 4, 37077 Göttingen, Germany

[‡]Max-Planck-Institute for Biophysical Chemistry, Am Fassberg 11, 37077 Göttingen, Germany

[§]Faculty of Chemistry and Chemical Biology, TU Dortmund University, Otto-Hahn-Straße 6, 44227 Dortmund, Germany

Supporting Information

ABSTRACT: Photon-powered charge separation is achieved in a supramolecular architecture based on the dense packing of functional building blocks. Therefore, self-assembled dimers of interpenetrated coordination cages consisting of redoxactive chromophors were synthesized in a single assembly step starting from easily accessible ligands and Pd(II) cations. Two backbones consisting of electron rich phenothiazine (PTZ) and electron deficient anthraquinone (ANQ) were used to assemble either homo-octameric or mixed-ligand double cages. The electrochemical and spectroscopic properties of the pure cages, mixtures of donor and acceptor cages and the mixed-ligand cages were compared by steady-state UV–vis and transient absorption spectroscopy, supported by cyclic voltammetry and spectroelectrochemistry. Only the mixed-ligand cages, allowing close intra-assembly communication between the donors and acceptors, showed the evolution of characteristic PTZ radical cation and ANQ radical anion features upon excitation in the transient spectra. In contrast, excitation of the mixtures of the homo-octameric donor and acceptor cages in solution did not lead to any signs of electron transfer. Densely packed photo- and redox-functional self-assemblies promise molecular-level control over the morphology of the charge separation layer in future photovoltaic applications.

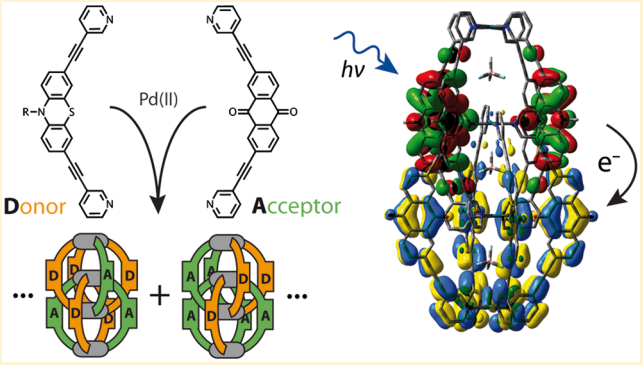

INTRODUCTION

Driven by the needs for alternative energy sources, the interaction of light with matter with the aim to capture solar energy has become a major research objective in chemistry.[1] In particular the area of organic photovoltaics has gained in importance in recent years. Part of this increasing interest is based on the elucidation of the details of the light-harvesting and electron-transfer systems in plants and photosynthetic bacteria. Many artificial photovoltaic cells are designed to convert solar energy into electric energy by mimicking the natural photophysical and photochemical processes.[2] The use of organic molecules or polymers is advantageous due to the large number of synthetic derivatization methods that can be employed to tune their absorption properties and electrochemical potential.[3] Although still suffering from lower efficiency compared to their inorganic counterparts,[4] organic solar cells bring some advantages, such as low-energy and low-cost production, versatility and flexibility in application.[5] One energy conversion strategy is based on the photoinduced generation of long-lived charge separation states. Therefore, several potent donor–acceptor ensembles varying from triarylamines or oligothiophenes[6] to porphyrine derivatives[7] combined with electron poor aromatic systems[8] or carbon nanomaterials[9] have been employed. On the other hand, dye-sensitized solar cells based on direct interfacial electron injection from excited chromophores, often ruthenium complexes,[10] have reached impressive performance.[11] Recently, solid-state hybrid solar cells based on perovskite materials were introduced as new low-cost competitors.[12]

A major challenge in the construction of efficient photovoltaic devices based on organic compounds is gaining control over the morphology of the photoactive layer with respect to the intermolecular contacts between the donor, acceptor and electrode materials.[13] In heterojunction solar cells, the arrangement of donors and acceptors must be designed in a way that the distance between them does not exceed the exciton diffusion length.[14] Several supramolecular approaches have been used to adjust the spatial arrangement of the components.[15]

Supramolecular self-assembly techniques have proven to be of particular utility for the precise arrangement of functional

Received: May 4, 2016
Published: June 3, 2016

DOI: 10.1021/jacs.6b04609
J. Am. Chem. Soc. 2016, 138, 8279–8287

building blocks.[16] The use of reversible connectivity such as noncovalent interactions or metal-coordination allows for a simple access to highly complex structures with self-healing properties. A variety of supramolecular systems with redox properties has been reported, including self-assembled rings,[17] cages,[18] grids, and others.[19]

Besides these rather simple architectures, topologically more complex assemblies such as catenanes, knots, ravels and other interpenetrated structures have been created in recent years.[20] In our opinion, entangled structures make interesting new materials for photovoltaic applications since their usually dense arrangement of individual components should allow for efficient electronic communication.

On the way to new materials for photovoltaic applications, a variety of discrete supramolecular donor−acceptor systems has been studied in the context of photoinduced charge transfer.[7,21] Examples include metallacycles reported by Stang et al.,[22] redox-addressable catenanes from the Stoddart group,[23,24] hydrogen-bonded assemblies by De Cola et al.,[25] self-assembled fibers from Würthner, Meijer, and co-workers,[26] and various inclusion compounds capable of host-to-guest charge transfer as reported by Fukuzumi et al.,[27] Sessler et al.,[28] Fujita et al.,[29] Würthner et al.[18c] and others.[30] A remarkable example of a prismatic coordination cage consisting of Zn-porphyrin donors and perylene bisimide acceptors was examined by Ballester and Flamigni.[31]

Herein, we report a novel supramolecular donor−acceptor system based on a combination of the concepts of metal-mediated self-assembly of coordination cages[32] and dense packing by topological interlocking.[20] We demonstrate that a previously described interpenetrated double-cage consisting of eight phenothiazine (PTZ) donors and four Pd(II) nodes[33] does survive 8-fold oxidation without imminent degradation, despite increasing its formal charge from +5 to +13 in the course of this process. We further introduce a new acceptor ligand based on anthraquinone (ANQ) and demonstrate its capability to form either homo-octameric double-cages or mixed-ligand dimers when combined with its PTZ counterpart. Phenothiazine and anthraquinone combinations are attractive redox systems because of their reversible and tunable oxidation/reduction potentials.[34] Intramolecular photoinduced charge transfer (PCT) based on this combination has been successfully demonstrated in the past, for example in a covalently bound dyad reported by Müller,[34g] but not yet in a self-assembly context. With the herein described approach, we show that light-induced charge transfer only occurs in systems containing both the donor and the acceptor in the same assembly, whereas mixtures of homomeric donors and acceptors do not show this effect in solution.

RESULTS AND DISCUSSION

Supramolecular Design. The double cage motif $[Pd_4L_8]$ is readily assembled by mixing banana-shaped bismonodentate pyridyl ligands of an appropriate donor angle and length with square-planar Pd(II) cations in a 2:1 ratio.[35] Double cages based on different backbones such as dibenzosuberone,[35b] carbazole,[35f] and acridone[35g] were previously studied with respect to their stimuli-responsive guest encapsulation features. Besides this, we introduced a series of double cages based on phenothiazine and its *S* mono- and dioxygenated derivatives and studied their rich redoxchemistry.[33] There, we could already show that the close packing of eight redox functionalities in the interpenetrated double cages leads to accelerated disproportionation of PTZ radical cationic sites as compared to the behavior of individual ligands in solution.

Here, we extend our repertoire of redox-active double cages by an electron deficient member comprising an anthraquinone backbone, that is of similar length and shape as phenothiazine. Based on our recent observations that (1) double cages can incorporate more than one kind of ligand as long as they are of comparable size and (2) preformed homomeric double cages are kinetically hindered from exchanging ligands when mixed in solution,[36] we are now able to compare the photo- and redox-properties of the following systems: (i) pure solutions of either double cage species, (ii) mixtures of homomeric double cages, and (iii) mixed-ligand double cages existing as mixtures of all statistical combinations and stereoisomers (Scheme 1).

Scheme 1[a]

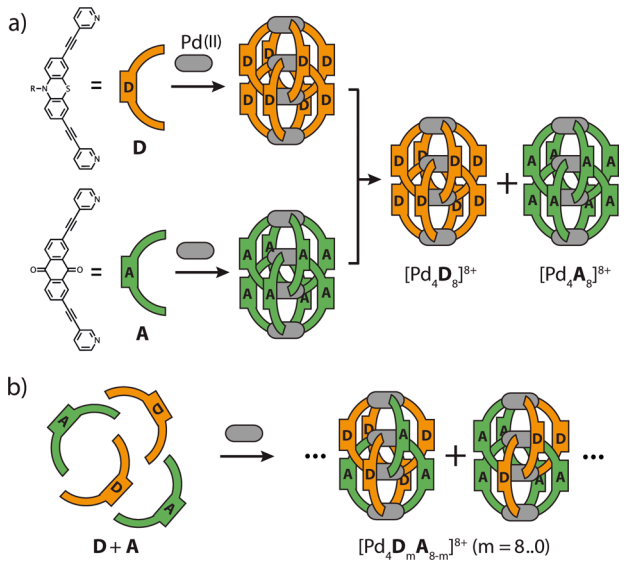

[a](a) Mixture of homo-octameric double cages $[Pd_4D_8]^{8+}$ and $[Pd_4A_8]^{8+}$ constructed from individual ligands **D** and **A** and $[Pd(CH_3CN)_4](BF_4)_2$ as metal source. (b) Mixed-ligand double cages $[Pd_4D_mA_{8-m}]^{8+}$ (m = 8...0) constructed from a solution of both ligands **D** and **A** mixed in a ratio of 1:1 and $[Pd(CH_3CN)_4](BF_4)_2$ as metal source. The ligands in $[Pd_4D_mA_{8-m}]^{8+}$ are statistically distributed. Anions inside pockets as well as counter anions have been omitted for clarity.

Synthesis and Characterization. The synthesis of ligand **D** and its corresponding double cage $[Pd_4D_8]^{8+}$ has been reported before.[33] The new ANQ ligand derivatives **A′** and **A** were prepared in four and seven steps, respectively, starting with the nitration and concomitant oxidation of anthrone, followed by reduction of the nitro groups and subsequent Sandmeyer reaction to give an anthraquinone backbone with two bromide substituents installed on the same side (Scheme 2). Sonogashira cross-coupling with 3-ethynylpyridine (for **A′**) or 3-ethynyl-5-(2-(2-methoxyethoxy)ethoxy)pyridine (for **A**) gave the desired ligands. The modified ethynylpyridine building block containing a polyethylene glycol chain was designed to enhance solubility in acetonitrile. The successful synthesis of both ligands **A′** and **A** was confirmed via ^{1}H NMR spectroscopy (Figure 1a and c).

Although anthraquinone ligands **A′** and **A** themselves are not soluble in acetonitrile, heating the ligands with 0.5 equiv of $[Pd(CH_3CN)_4](BF_4)_2$ at 70 °C for 12 h in acetonitrile resulted

DOI: 10.1021/jacs.6b04609
J. Am. Chem. Soc. 2016, 138, 8279−8287

Scheme 2. Synthetic Route to the Ligands A′ and A[a]

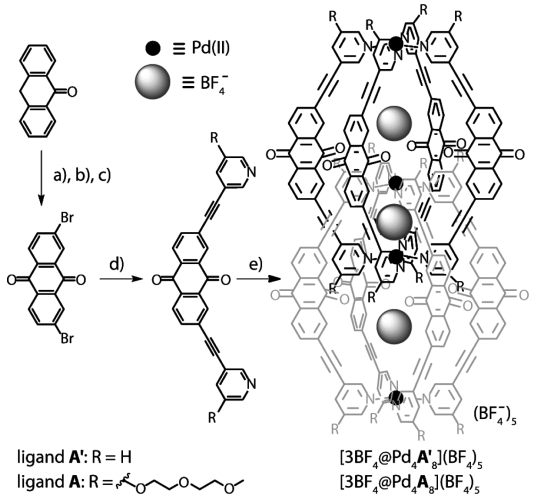

[a](a) fuming HNO_3, acetic acid; (b) Na_2S, NaOH, EtOH/H_2O; (c) CuBr, $tBuNO_2$, HCl; (d) CuI, $Pd(PPh_3)_2Cl_2$, NEt_3, 3-ethynylpyridine or 3-ethynyl-5-(2-(2-methoxyethoxy)ethoxy)-pyridine. Self-assembly to the double cages $[3BF_4@Pd_4A'_8](BF_4)_5$ and $[3BF_4@Pd_4A_8](BF_4)_5$; (e) $[Pd(CH_3CN)_4](BF_4)_2$, CD_3CN, 70 °C.

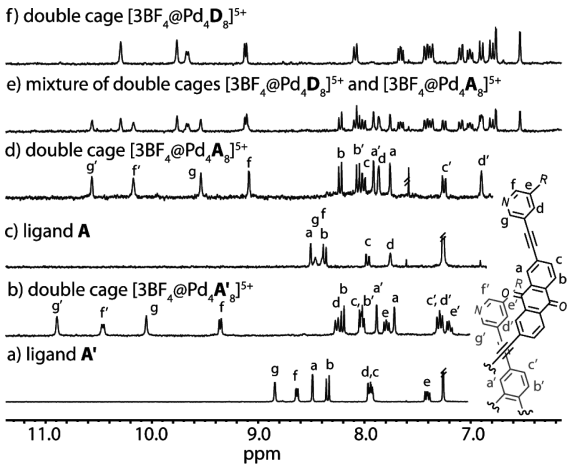

Figure 1. ^{1}H NMR spectra (300 MHz, 298 K) of (a) ligand **A′** ($CDCl_3$); (b) double cage $[3BF_4@Pd_4A'_8]^{5+}$ (CD_3CN); (c) ligand **A** ($CDCl_3$); (d) double cage $[3BF_4@Pd_4A_8]^{5+}$ (CD_3CN); (e) mixture of homo-octameric double cages $[3BF_4@Pd_4D_8]^{5+}$ and $[3BF_4@Pd_4A_8]^{5+}$ in a ratio of 1:1 (CD_3CN); (f) double cage $[3BF_4@Pd_4D_8]^{5+}$ (CD_3CN).

in the quantitative formation of the interpenetrated double cages as could be confirmed by ^{1}H NMR spectroscopy (Figure 1b and d) and high resolution mass spectrometry (Figures SI-4 and SI-12). The assembly of ligands into the double cage structure causes a splitting of all ^{1}H NMR signals into two sets of equal intensity. Remarkably, the ^{1}H NMR signals of the pyridine entity show a strong downfield shift characteristic for coordination to the Pd(II) cation. The high resolution ESI mass spectra revealed the presence of penta-, tetra- and tricationic species with different numbers of counteranions, verifying the formation of interpenetrated double cages.

Since no crystals suitable for X-ray structure analysis could be obtained, we prepared a DFT (ωB97XD/def2-SVP) model of the double cage $[3BF_4@Pd_4A'_8]^{5+}$ (Figure SI-15). The calculation reveals a highly symmetric structure with three cavities for the uptake of anions. The Pd−Pd distances for the outer pockets and for the inner pocket are in agreement with the distances reported for similar double cages.[35]

The mixture of cages $[3BF_4@Pd_4D_8]^{5+}$ and $[3BF_4@Pd_4A_8]^{5+}$ was prepared by mixing acetonitrile solutions of the preassembled double cages in a ratio of 1:1. Figure 1e shows the ^{1}H NMR spectrum of the mixture of homo-octameric double cages $[3BF_4@Pd_4D_8]^{5+}$ and $[3BF_4@Pd_4A_8]^{5+}$. The signals of both cages are clearly distinguishable and can be assigned to individual cage protons (compare Figure 1d–f), showing that both species can coexist as a metastable mixture in solution without exchanging ligands at significant rates. Indeed, the thermodynamic product of this mixture of two cages is a mixed-ligand cage with a statistical distribution of ligands as could be shown previously for mixed cages based on similar ligand sizes.[36] An ESI high resolution mass spectrum of the mixture of double cages $[3BF_4@Pd_4D_8]^{5+}$ and $[3BF_4@Pd_4A_8]^{5+}$ shows clear signals for the distinct double cage species and no signals for species with exchanged ligands, confirming the kinetic stability of the homo-octameric double cages (Figure 2a).

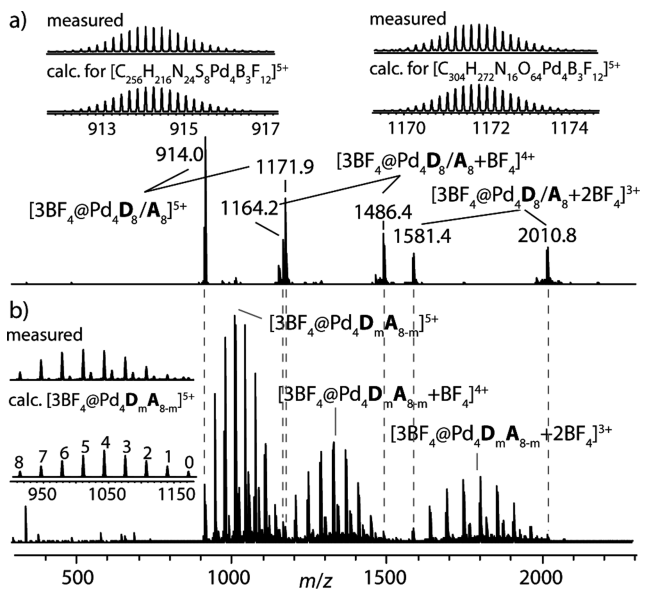

Figure 2. ESI mass spectra of (a) mixture of homo-octameric double cages $[3BF_4@Pd_4D_8]^{5+}$ and $[3BF_4@Pd_4A_8]^{5+}$ in a ratio of 1:1 and (b) mixed-ligand double cages $[3BF_4@Pd_4D_mA_{8-m}]^{5+}$ (m = 8...0) with statistical distribution of ligands.

The mixed-ligand cages $[3BF_4@Pd_4D_mA_{8-m}]^{5+}$ (m = 8...0) were synthesized by mixing first the ligands **D** and **A** in a ratio of 1:1 and then adding $[Pd(CH_3CN)_4](BF_4)_2$ in acetonitrile. The solution was heated to 70 °C for 12 h. The ^{1}H NMR spectrum of the mixed-ligand cages shows very broad signals due to the distribution of both ligand types within the cages and hence numerous different proton environments (Figures SI-7 and SI-14). The ESI high resolution mass spectrum of the mixed-ligand cages clearly identifies the components of the mixture as the expected statistical distribution $[3BF_4@Pd_4D_mA_{8-m}]^{5+}$ (m = 8...0) of fully intact double cages (Figure 2b).

UV–Vis Absorption Spectroscopy. The ground-state absorption spectra of the double cages in acetonitrile show two main absorption maxima (Figure 3). The first maximum around

DOI: 10.1021/jacs.6b04609
J. Am. Chem. Soc. 2016, 138, 8279–8287

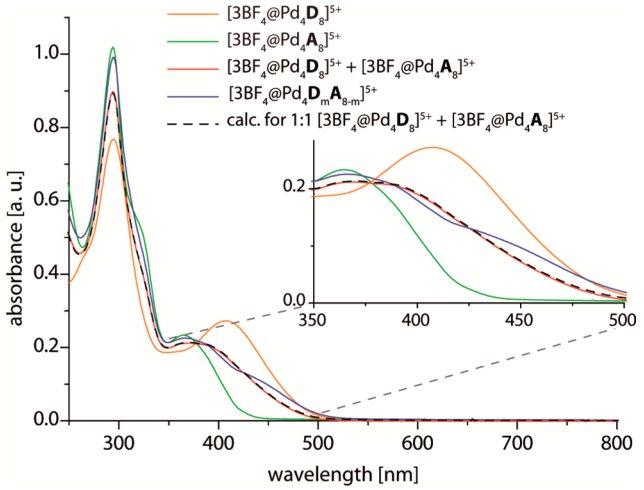

Figure 3. UV−vis spectra of double cages $[3BF_4@Pd_4\mathbf{D}_8]^{5+}$ (20 μM in CH_3CN, orange line) and $[3BF_4@Pd_4\mathbf{A}_8]^{5+}$ (20 μM in CH_3CN, green line), their mixture (10 μM each in CH_3CN, red line), and mixed-ligand double cages $[3BF_4@Pd_4\mathbf{D}_m\mathbf{A}_{8-m}]^{5+}$ with m = 8...0 (20 μM in CH_3CN, blue line). The spectrum for the mixture of homo-octameric double cages (dashed black line) in a ratio of 1:1 can be superimposed with the sum of the double cage spectra (cuvette path length: 0.1 cm in all cases).

295 nm is dominated by intraligand $\pi-\pi^*$ transitions. The second absorption maximum is broad and appears at 408 nm for $[3BF_4@Pd_4\mathbf{D}_8]^{5+}$ and 365 nm for $[3BF_4@Pd_4\mathbf{A}_8]^{5+}$. The steady-state UV−vis measurements unambiguously indicate electronic communication between the ligand chromophores within the mixed-ligand cage structure $[3BF_4@Pd_4\mathbf{D}_m\mathbf{A}_{8-m}]^{5+}$ (m = 8...0). The absorption spectrum of the mixed cages substantially differs, especially in the region from 350 to 500 nm, from the sum of the absorption spectra of its components. In contrast, the spectrum of the mixture of homo-octameric cages $[3BF_4@Pd_4\mathbf{D}_8]^{5+}$ and $[3BF_4@Pd_4\mathbf{A}_8]^{5+}$ can be perfectly reconstructed from the sum of the spectra of each cage in a ratio of 1:1.

Chemical Oxidation of $[3BF_4@Pd_4\mathbf{D}_8]^{5+}$. The utilization of the double-cage architecture in photoinduced charge transfer processes requires to confirm the robustness of the self-assembled system in the involved redox processes. This is of particular importance for the donor components, since oxidation leads to an increase of the positive charge of the already cationic coordination cage, thereby risking a Coulomb driven disintegration. We therefore examined the stability of the double cage $[3BF_4@Pd_4\mathbf{D}_8]^{5+}$ upon chemical oxidation and rereduction, monitored by ^{1}H NMR and UV−vis spectroscopy. For this, all eight donors in double cage $[3BF_4@Pd_4\mathbf{D}_8]^{5+}$ were stoichiometrically oxidized with $[Fe(III)bpy_3](BF_4)_3$ in acetonitrile solution (see titration in Figure SI-19). Figure 4a shows the UV−vis spectrum after the first oxidation (the spectrum of the formed $[Fe(II)bpy_3]^{2+}$ cation has been subtracted). New bands in the visible region of the spectrum appear after oxidation: one sharp peak with maximum at 525 nm and a very broad peak with maximum around 680 nm. These bands are characteristic for the absorption of the radical cation of phenothiazine and are assigned to cage species containing up to eight oxidized ligands ($[3BF_4@Pd_4\mathbf{D}^{(\bullet+)}_8]^{13+}$). During the oxidation process, the color of the solution changed from yellow to dark brown. After oxidation, Zn powder was added to the solution in order to fully reduce the radical species back to

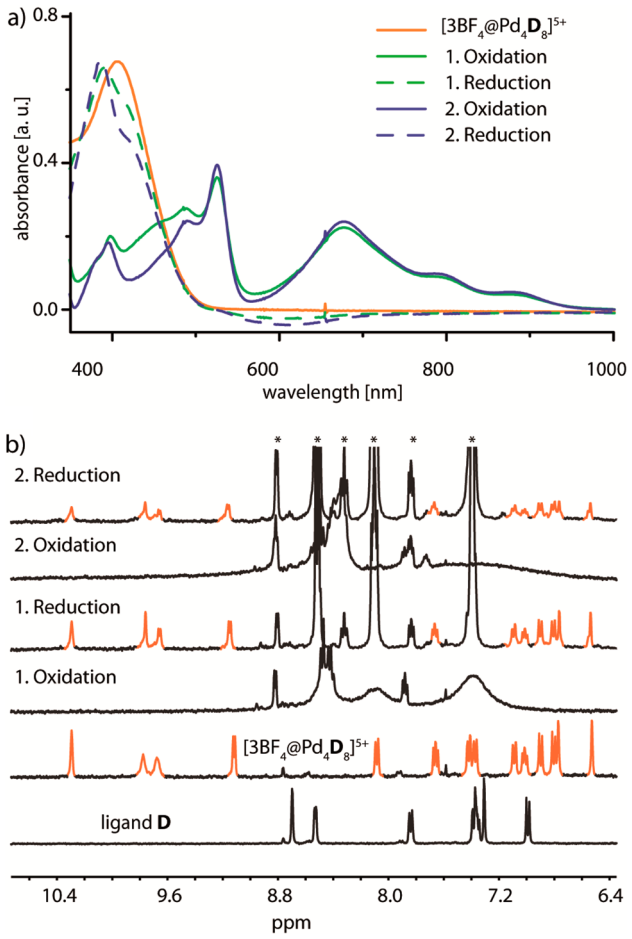

Figure 4. Chemical oxidation of double cage $[3BF_4@Pd_4\mathbf{D}_8]^{5+}$ in acetonitrile with $[Fe(III)(bpy)_3](BF_4)_3$ and subsequent rereduction with Zn powder monitored by (a) UV−vis spectroscopy (the spectrum of $[Fe(II)(bpy)_3](BF_4)_2$ was subtracted) and (b) ^{1}H NMR spectroscopy (double cage signals in orange, 400 MHz, 298 K, CD_3CN). Asterisk (*) denotes signals coming from $[Fe(II)(bpy)_3](BF_4)_2$ and free bpy.

the double cage $[3BF_4@Pd_4\mathbf{D}_8]^{5+}$. As expected, the bands above 500 nm vanished and the band around 400 nm was recovered overlapping with a new band at 387 nm. This new band indicates a partial S oxygenation of the oxidized double cage during the course of the experiment by reaction with residual water as has been shown previously.[33] The second oxidation/reduction cycle shows a similar behavior as the first one which allows us to conclude that the majority of the double cages survive the repeated oxidation and reduction rounds in a time window of about 10 min per cycle.

Further proof for the survival of the double cage upon oxidation was made by monitoring the process with ^{1}H NMR spectroscopy (Figure 4b). As expected, after oxidation all signals for the paramagnetic double cage $[3BF_4@Pd_4\mathbf{D}^{(\bullet+)}_8]^{13+}$ disappear from the spectrum. The unique NMR signature of the double cage is clearly recovered upon rereduction with Zn powder. The process can be repeated in cycles several times. Although intensity losses of the cage signals with each oxidation/reduction cycle also point to a creeping decomposition or oxygenation during the oxidation/reduction cycles, a significant ratio of the cages survives these relatively harsh conditions. The accumulation of oxygenation products after each cycle was also confirmed by ESI mass spectrometry

DOI: 10.1021/jacs.6b04609
J. Am. Chem. Soc. 2016, 138, 8279−8287

(Figure SI-22). Most interestingly, no destruction of the double cage to smaller fragments or even release of free ligand was indicated in the spectra. It is further worth noting, that these experiments exclude the possibility of a concomitant oxidation-induced disassembly and reduction-induced reassembly of the double cages, since (i) the UV trace of the oxidized cage differs from that of the oxidized free ligand and (ii) the formation of double cages from free ligands is known to be much slower than the duration of the conducted oxidation/rereduction experiment.

Cyclic Voltammetry. Both phenothiazine and anthraquinone are known to undergo well-defined, reversible oxidation and reduction processes. To probe the effects of self-assembly on the redox chemistry, CV measurements were performed (Figures 5 and SI-23). The voltammograms for the donor-based double cage $[3BF_4@Pd_4\mathbf{D}_8]^{5+}$ as well as for the free ligand **D** show a quasi-reversible redox peak. The oxidation peak of the double cage is shifted to more positive potential compared to the free ligand (+0.13 V in CH_3CN and +0.12 V in CH_2Cl_2). This can be attributed to the coordination of the donors to the cationic Pd(II) centers. A second oxidation occurs at higher potential and is irreversible. Although the acceptor-based double cage $[3BF_4@Pd_4\mathbf{A}_8]^{5+}$ has an acceptable solubility in pure acetonitrile, addition of large amounts of electrolyte salt was found to cause substantial precipitation. Therefore, both the double cage and the ligand were electrochemically characterized in CH_2Cl_2. Both compounds exhibit two quasi-reversible redox waves. The first reduction wave of the double cage $[3BF_4@Pd_4\mathbf{A}_8]^{5+}$ is shifted by 0.10 V and the second by 0.14 V to more negative potential compared to the free ligand.

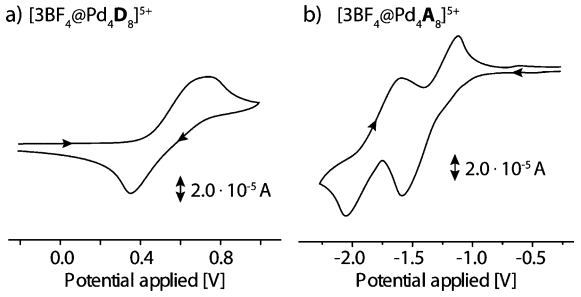

Figure 5. Cyclic voltammograms of (a) $[3BF_4@Pd_4\mathbf{D}_8]^{5+}$ and (b) $[3BF_4@Pd_4\mathbf{A}_8]^{5+}$ (1 mM in CH_2Cl_2, recorded at a glassy carbon working electrode against a $Ag/AgNO_3$ [10 mM] reference electrode, diagram referenced against Fc/Fc^+, supporting electrolyte: 0.1 M $[NBu_4][PF_6]$, scan rate: 100 mV·s^{-1}).

The observed redox potentials of the statistical combination of the mixed-ligand double cages $[3BF_4@Pd_4\mathbf{D}_m\mathbf{A}_{8-m}]^{5+}$ appear at the same positions as measured for each of the homo-octameric double cages (Table 1), thus demonstrating that the donors and acceptors do not exhibit strong electrochemical communication within the cage architecture in the electronic ground state. The data of Table 1 can be inserted into the Rehm–Weller equation $\Delta G_{PCT} = E_{ox} - E_{red} - \Delta E_{00} - \Delta G_C$ to estimate the free energy for PCT in the mixed ligand cage.[37] ΔE_{00} = 2.7 eV was derived from the intersection of the normalized absorption and emission spectra of **D** which is lower in energy than for **A**.[33] The Coulomb term amounts to ΔG_C = 0.08 eV for an estimated charge separation of 5 Å. Hence photoinduced electron transfer in the mixed ligand cage is driven by a net gain in free energy of ΔG_{PCT} = −0.84 eV.

Table 1. Cyclic Voltammetry Parameters[a]

compd	E_{ox} [V]	E_{red1} [V]	E_{red2} [V]
ligand **D**	0.39[b]		
	0.41[c]		
$[3BF_4@Pd_4\mathbf{D}_8]^{5+}$	0.52[b]		
	0.53[c]		
ligand **A**		−1.25[c]	−1.70[c]
$[3BF_4@Pd_4\mathbf{A}_8]^{5+}$		−1.35[c]	−1.84[c]
$[3BF_4@Pd_4\mathbf{D}_m\mathbf{A}_{8-m}]^{5+}$	0.48[c]	−1.30[c]	−1.72[c]

[a]All values are given in reference to Fc/Fc^+. [b]Measurements were performed in dry CH_3CN. [c]Measurements were performed in dry CH_2Cl_2.

Spectroelectrochemistry. Although chemical oxidation enabled us to obtain the absorption spectrum of the oxidized $[3BF_4@Pd_4\mathbf{D}^{(\bullet+)}{}_8]^{13+}$ double cage species (see above), the UV–vis spectrum is complicated by waste products resulting from the reaction. In addition, attempts to chemically reduce the acceptor-based double cage $[3BF_4@Pd_4\mathbf{A}_8]^{5+}$ proofed to be difficult. For this reason, we performed spectroelectrochemical measurements to characterize the oxidized and reduced donor and acceptor cages, respectively. A thin layer cell (1 mm optical path length) including a Pt gauze and a $Ag/AgNO_3$ reference electrode was used in combination with a diode array spectrophotometer. The observed absorption spectrum of oxidized $[3BF_4@Pd_4\mathbf{D}^{(\bullet+)}{}_8]^{13+}$ is very similar to the one obtained by chemical oxidation (Figures SI-26 and SI-30), showing one sharp peak around 525 nm and one very broad peak around 680 nm.[38] The spectrum of the reduced double cage $[3BF_4@Pd_4\mathbf{A}^{(\bullet-)}{}_8]^{3-}$ shows an appearance of a broad absorption band around 700 nm (Figure SI-28). The spectra of the oxidized or reduced mixed-ligand cage $[3BF_4@Pd_4\mathbf{D}_m\mathbf{A}_{8-m}]$ are very similar (Figure SI-29) to those obtained for the homo-octameric double cages, thus confirming the results from cyclic voltammetry that the donors and acceptors in the mixed cages are individually addressable in the ground state.

Transient Absorption Spectroscopy. Next, we applied femtosecond pump–probe spectroscopy to get time-resolved insights into the processes following the photoexcitation of the homomeric cages, their mixture as well as the mixed-ligand cages. Pump pulses in the range 385–440 nm were used covering the absorption bands of electron acceptor and donor (Figure 3). Light-induced processes were probed in the UV–vis between 350 and 730 nm by measuring transient absorption changes using a white-light continuum (for experimental details, see the Supporting Information).

Figure 6 shows the result of the transient absorption spectroscopic studies for the excitation of the mixed-ligand cage $[3BF_4@Pd_4\mathbf{D}_m\mathbf{A}_{8-m}]^{5+}$ in comparison to the results obtained from the spectroelectrochemical experiments of the oxidized $[3BF_4@Pd_4\mathbf{D}^{(\bullet+)}{}_8]^{13+}$ and reduced $[3BF_4@Pd_4\mathbf{A}^{(\bullet-)}{}_8]^{3-}$ species.[38] The absorption spectrum of the mixed-ligand cage shows a similar absorption pattern as the sum of radicals of the homogeneous donor and acceptor cages, thus delivering a first indication for the light-induced formation of a charge separated state.

The free acceptor and donor ligands and the corresponding homogeneous cages $[3BF_4@Pd_4\mathbf{A}_8]^{5+}$ and $[3BF_4@Pd_4\mathbf{D}_8]^{5+}$ were investigated in separate experiments. Consistent with the literature, the fluorescence of the free arylethynyl substituted anthraquinone ligand is weak and shows a strong Stokes shift of ∼6000 cm^{-1} indicating charge-transfer character

DOI: 10.1021/jacs.6b04609
J. Am. Chem. Soc. 2016, 138, 8279–8287

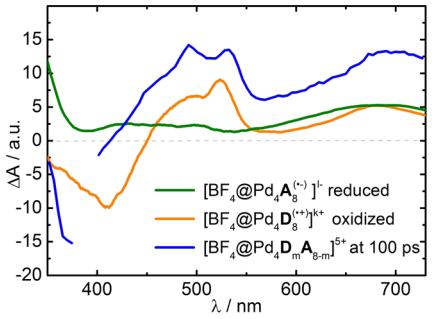

Figure 6. Electrochemically generated difference absorption spectra for the oxidized $[3BF_4@Pd_4\mathbf{D}^{(\bullet+)}{}_8]$ and reduced $[3BF_4@Pd_4\mathbf{A}^{(\bullet-)}{}_8]$ species are compared with a transient absorption spectrum measured 100 ps after 385 nm excitation of the mixed-ligand cage $[3BF_4@Pd_4\mathbf{D}_m\mathbf{A}_{8-m}]^{5+}$ (m = 8...0).

of the emitting state.[39] The time dependence of the transient spectra of **A** presented in Figure 7a exhibits the conversion of

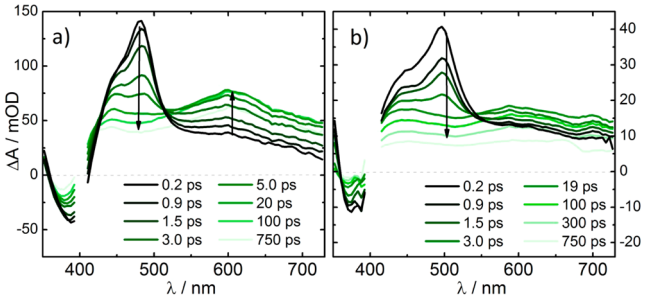

Figure 7. Transient difference spectra of (a) the free anthraquinone electron acceptor ligand **A** and (b) the homogeneous double cage $[3BF_4@Pd_4\mathbf{A}_8]^{5+}$ at selected pump−probe delays (regions obscured by the pump wavelength at λ_{pump} = 400 nm were cut out).

an excited state absorption with a maximum at 480 nm created within the duration of the excitation pulse into a broad feature centered at 600 nm. In agreement with previous studies revealing efficient intersystem crossing as the dominant relaxation channel of photoexcited anthraquinone and its derivatives,[34g,39,40] we associate the corresponding time constant of τ_{S1} = (2.4 ± 0.2) ps to the transformation of the excited singlet into a long-lived triplet state. Interestingly, the photophysics of the anthraquinone ligand is almost unaffected when the ligand is assembled in the cage $[3BF_4@Pd_4\mathbf{A}_8]^{5+}$. This follows from Figure 7b which shows for the double cage apart from small spectral shifts (the maximum of the singlet state absorption band now appears at 500 nm) almost identical time-dependent transients as the free ligand in Figure 7a. A closer analysis of Figure 7b indicates that excitation of $[3BF_4@Pd_4\mathbf{A}_8]^{5+}$ leads to a long-lived triplet state within τ_{S1} = (2.2 ± 0.2) ps.

Similar to the acceptor ligand, the fluorescence spectrum of the free phenothiazine donor ligand shows a strong Stokes shift, in this case amounting to ~5700 cm^{-1}.[33] The origin of this shift is probably a charge transfer character of the emitting state because the transient spectra depicted in Figure 8a showed a red-shift and narrowing of the stimulated emission component. Only at pump−probe delays >20 ps the stimulated emission component (superimposed by strong excited state absorption) assumes the shape of the fluorescence spectrum. The formation of the charge transfer state can be described by two

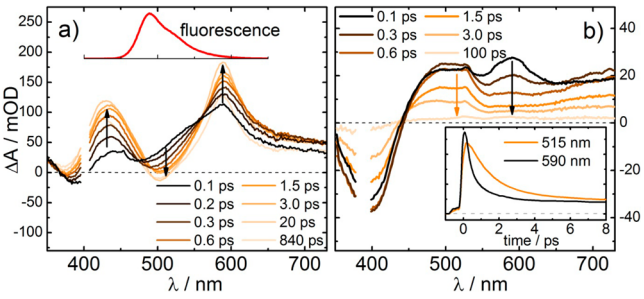

Figure 8. Transient absorption spectra of (a) the free phenothiazine electron donor ligand **D** (the stationary fluorescence spectrum of **D** is shown for comparison, exc. 400 nm) and (b) the homogeneous double cage $[3BF_4@Pd_4\mathbf{D}_8]^{5+}$ at selected pump−probe delays (the inset shows time-dependent traces at 515 and 590 nm).

exponentials with time constants of 0.3 ± 0.05 ps and 7.6 ± 1.0 ps, its lifetime is >3 ns. Similar nanosecond singlet lifetimes have been reported for other phenothiazine derivatives.[34g,41]

The photo reactivity of the phenothiazine donor completely changes when it is bound in the palladium double cage $[3BF_4@Pd_4\mathbf{D}_8]^{5+}$. The steady-state fluorescence spectrum observed for free **D** is entirely quenched in the cage complex. Shortly after the pump pulse the transient absorption spectrum of $[3BF_4@Pd_4\mathbf{D}_8]^{5+}$ indicates some evidence of the phenothiazine excited singlet state characterized by the peak at 590 nm as illustrated in Figure 8b. But this feature disappears with a time constant of about 200 fs and absorption bands with maxima at 500 and 700 nm remain. A comparison of the 3.0 ps transient with spectra of the chemically or electrochemically oxidized double cage (Figures 4a and 6, respectively) shows striking similarities. Moreover, excitation of phenothiazine in the presence of transition metal ions is well-known to produce phenothiazine radical cations by efficient electron transfer.[42] Hence, we attribute the photoinduced dynamics of $[3BF_4@Pd_4\mathbf{D}_8]^{5+}$ to a subpicosecond ligand-to-metal electron transfer to the bound Pd(II) cations. Note that unlike (electro-)chemical oxidation of the donor double cage leading at the extreme to $[3BF_4@Pd_4\mathbf{D}_8{}^{(\bullet+)}]^{13+}$ photoexcitation produces only a single exciton which after subsequent CT reacts formally to the proposed compound $[3BF_4@Pd^{II}{}_3\mathbf{D}_7Pd^{I}\mathbf{D}^{(\bullet+)}]^{5+}$ with one phenothiazine radical cation, one palladium in oxidation state +1, and unchanged total charge. This difference can easily explain small variations between the radical cation absorption spectra appearing in Figures 4a, 6, and 8b. The insert in Figure 8b shows that the lifetime of the CT state is only short. The dominant contribution associated with the decay of the phenothiazine radical cation absorption at 500 nm due to back electron transfer has a time constant of τ_{CT} = (1.3 ± 0.1) ps.

Transient absorption spectra of mixed-ligand cages $[3BF_4@Pd_4\mathbf{D}_m\mathbf{A}_{8-m}]^{5+}$ (m = 0...8) were generated with pump pulses at 385 nm where both donor and acceptor are excited with almost equal probability (55% and 45%, respectively; Figure 9a). Accordingly, these spectra show evidence of the initially excited chromophore singlet states at 500 (anthraquinone) and 590 nm (phenothiazine) directly after excitation (cf. Figures 7 and 8). These features disappear within 200 fs, and for longer delay times spectral signatures of the phenothiazine radical cation arise at 500 and 700 nm. Compared to the homogeneous donor cage $[3BF_4@Pd_4\mathbf{D}_8]^{5+}$ exhibiting $\mathbf{D}^{\bullet+}$ production in a ligand-to-metal charge transfer (Figure 8b), the transient spectra of the excited mixed-ligand cage show enhanced amplitude around

DOI: 10.1021/jacs.6b04609
J. Am. Chem. Soc. 2016, 138, 8279−8287

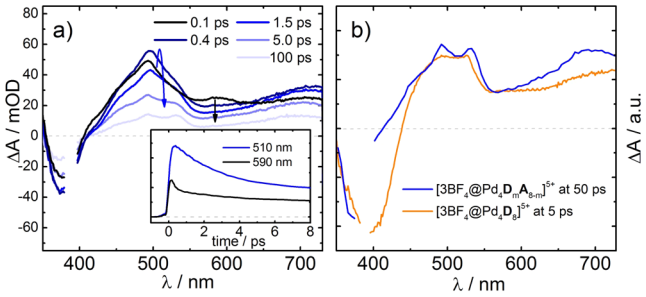

Figure 9. (a) Transient absorption spectra of the mixed-ligand cage $[3BF_4@Pd_4\mathbf{D}_m\mathbf{A}_{8-m}]^{5+}$ (m = 8...0) at selected pump−probe delays (the inset shows time traces at 510 and 590 nm). (b) Scaled transients of the mixed-ligand cage and the homogeneous donor cage $[3BF_4@Pd_4\mathbf{D}_8]^{5+}$ are compared.

700 nm (Figure 9b). As clarified in Figure 6, this observation suggests the formation of the anthraquinone radical anion $\mathbf{A}^{\bullet-}$ which is characterized by a broad absorption band at 700 nm. Hence, we attribute the observed <200 fs dynamics in the photoexcited mixed double cages to an electron transfer reaction from the phenothiazine donor to the anthraquinone acceptor ligand (DA-CT) independent of which chromophore is excited. In contrast, control experiments with a 1:1 mixture of the homo-octameric donor and acceptor cages in acetonitrile solution did not provide any evidence for a DA-CT process. In this case, the pump−probe absorption spectrum (Figure SI-31) consists of a weighted sum of the individual homomeric components which significantly differs from the mixed-ligand cage signal.

A closer analysis of the decay of the $\mathbf{D}^{\bullet+}$ absorption band in Figure 9a requires at least three components. The dominant contributions with almost equal weight are characterized by time constants of 3.3 ps and >1.0 ns indicating a significantly higher stability of the DA-CT state than the ligand-to-metal CT state of $[3BF_4@Pd_4\mathbf{D}_8]^{5+}$. Recently a similar broad range of lifetimes were observed for the photoinduced charge separated state of a covalently linked PTZ-ANQ system, and it was proposed that after singlet excitation of the ANQ chromophore forward electron transfer to a singlet DA-CT state competes with intersystem crossing.[34g] Subsequent electron transfer starting from the triplet state forms a triplet charge separated diradical ion pair with a much longer lifetime than the singlet DA-CT due to spin restrictions. We cannot rule out that this mechanism forming singlet and triplet CT states is of relevance for our mixed-ligand cage, too. But it is also possible that the wide span of lifetimes is caused by the broad distribution of $[3BF_4@Pd_4\mathbf{D}_m\mathbf{A}_{8-m}]^{5+}$ complexes with different stoichiometry and/or stereo configurations.

CONCLUSIONS

In a one-step Pd-mediated self-assembly, we obtained a new supramolecular mixed-ligand coordination architecture which combines an electron donor and an electron acceptor part within one densely packed, interpenetrated double cage. A series of experiments allowed us to compare the electrochemical and photophysical behavior of these mixed-ligand cages with both of their homomeric relatives and a kinetically stable mixture of the latter ones.

UV−vis- and NMR-monitored oxidation reactions were conducted to show that the cationic double cage architecture survives the oxidation of up to all eight donor sites within a reasonable time window. The steady state UV−vis spectrum of the mixed-ligand cages indicates interaction between the donor and acceptor chromophors, whereas no signs for electronic communication between the donors and acceptors was observed during electrochemical characterization of the ground state species.

Pump−probe transient absorption spectroscopy revealed that only the mixed-ligand cages, which contain donors and acceptors in immediate vicinity, allow for the formation of a relatively stable charge separated state which shows spectroscopic features assignable to the sum of the donor radical cation and acceptor radical anion absorptions.

The supramolecular assembly approach based on interpenetrated cage architectures shown herein may spur the development of novel materials for photoactive layers with controlled morphology in future photovoltaic devices. Furthermore, the system's capability of reversible electron cycling between highly charged species and photoinduced charge transfer creates potential to support photo- and electrocatalytic processes. We are currently working on the selective assembly of mixed-ligand cages with ligands sitting on targeted positions, in order to overcome the intrinsic problems with statistical product mixtures. Thereby, we aim at gaining control over directed charge transfer processes by rational supramolecular design.

ASSOCIATED CONTENT

Supporting Information

The Supporting Information is available free of charge on the ACS Publications website at DOI: 10.1021/jacs.6b04609.

Experimental details and further MS, NMR, UV−vis, electrochemical and computational data (PDF)

AUTHOR INFORMATION

Corresponding Author

*guido.clever@tu-dortmund.de

Notes

The authors declare no competing financial interest.

ACKNOWLEDGMENTS

M.F. thanks the Evonik Foundation for PhD fellowship. We thank the FCI and the DFG (SFB 1073, project B05, and CL 489/2-1) for financial support, Dr. H. Frauendorf for measuring the ESI-MS spectra and Dr. M. John for help with NMR spectroscopy. We would like to thank Jana Lücken and Sonja Schmidt for their support in synthesis. We thank Prof. Dr. Shunichi Fukuzumi and Prof. Dr. Tomoyoshi Suenobu (Graduate School of Engineering, Osaka University) for their support and hospitality, fruitful discussions and experimental help with the chemical oxidation experiment.[33]

REFERENCES

(1) Lewis, N. S.; Nocera, D. G. *Proc. Natl. Acad. Sci. U. S. A.* **2006**, *103*, 15729−15735.
(2) Barber, J.; Tran, P. D. *J. R. Soc., Interface* **2013**, *10*, 20120984.
(3) (a) Günes, S.; Neugebauer, H.; Sariciftci, N. S. *Chem. Rev.* **2007**, *107*, 1324−1338. (b) Brabec, C. J.; Gowrisanker, S.; Halls, J. J. M.; Laird, D.; Jia, S.; Williams, S. P. *Adv. Mater.* **2010**, *22*, 3839−3856.
(4) Green, M. A.; Emery, K.; Hishikawa, Y.; Warta, W.; Dunlop, E. D. *Prog. Photovoltaics* **2016**, *24*, 3−11.
(5) (a) Spanggaard, H.; Krebs, F. C. *Sol. Energy Mater. Sol. Cells* **2004**, *83*, 125−146. (b) Kippelen, B.; Brédas, J.-L. *Energy Environ. Sci.* **2009**, *2*, 251−261. (c) Brédas, J.-L.; Norton, J. E.; Cornil, J.; Coropceanu, V.

DOI: 10.1021/jacs.6b04609
J. Am. Chem. Soc. 2016, 138, 8279−8287

Acc. Chem. Res. **2009**, *42*, 1691−1699. (d) Clarke, T. M.; Durrant, J. R. *Chem. Rev.* **2010**, *110*, 6736−6767. (e) Hoppe, H.; Sariciftci, N. S. *J. Mater. Res.* **2004**, *19*, 1924−1945.
(6) (a) Xu, T.; Yu, L. *Mater. Today* **2014**, *17*, 11−15. (b) Lambert, C.; Nöll, G. *Angew. Chem., Int. Ed.* **1998**, *37*, 2107−2110.
(7) (a) Wasielewski, M. R. *Chem. Rev.* **1992**, *92*, 435−461. (b) Wasielewski, M. R. *J. Org. Chem.* **2006**, *71*, 5051−5066. (c) Sessler, J. L.; Wang, B.; Harriman, A. *J. Am. Chem. Soc.* **1993**, *115*, 10418−10419. (d) Harriman, A.; Kubo, Y.; Sessler, J. L. *J. Am. Chem. Soc.* **1992**, *114*, 388−390.
(8) (a) Würthner, F.; Saha-Möller, C. R.; Fimmel, B.; Ogi, S.; Leowanawat, P.; Schmidt, D. *Chem. Rev.* **2016**, *116*, 962−1052. (b) Klein, J. H.; Schmidt, D.; Steiner, U. E.; Lambert, C. *J. Am. Chem. Soc.* **2015**, *137*, 11011−11021.
(9) (a) D'Souza, F.; Maligaspe, E.; Ohkubo, K.; Zandler, M. E.; Subbaiyan, N. K.; Fukuzumi, S. *J. Am. Chem. Soc.* **2009**, *131*, 8787−8797. (b) D'Souza, F.; Ito, O. *Chem. Commun.* **2009**, 4913−4928. (c) Bottari, G.; de la Torre, D.; Guldi, D. M.; Torres, T. *Chem. Rev.* **2010**, *110*, 6768−6816. (d) Bottari, G.; Trukhina, O.; Ince, M.; Torres, T. *Coord. Chem. Rev.* **2012**, *256*, 2453−2477. (e) Konishi, T.; Ikeda, A.; Shinkai, S. *Tetrahedron* **2005**, *61*, 4881−4899.
(10) (a) Laine, P. P.; Campagna, S.; Loiseau, F. *Coord. Chem. Rev.* **2008**, *252*, 2552−2571. (b) Wenger, O. S. *Coord. Chem. Rev.* **2015**, *282*−*283*, 150−158.
(11) (a) O'Regan, B.; Grätzel, M. *Nature* **1991**, *353*, 737−740. (b) Hagfeldt, A.; Boschloo, G.; Sun, L.; Kloo, L.; Pettersson, H. *Chem. Rev.* **2010**, *110*, 6595−6663.
(12) Snaith, H. J. *J. Phys. Chem. Lett.* **2013**, *4*, 3623−3630.
(13) Scharber, M. C.; Mühlbacher, D.; Koppe, M.; Denk, P.; Waldauf, C.; Heeger, A. J.; Brabec, C. J. *Adv. Mater.* **2006**, *18*, 789−794.
(14) Safont-Sempere, M. M.; Fernandez, G.; Würthner, F. *Chem. Rev.* **2011**, *111*, 5784−5814.
(15) (a) Wasielewski, M. R. *Acc. Chem. Res.* **2009**, *42*, 1910−1921. (b) Lista, M.; Areephong, J.; Sakai, N.; Matile, S. *J. Am. Chem. Soc.* **2011**, *133*, 15228−15231.
(16) (a) Steed, J. W.; Atwood, J. L. *Supramolecular Chemistry*, 2nd ed., Wiley: New York, 2009. (b) Diederich, F.; Stang, P. J.; Tykwinski, R. R. *Modern Supramolecular Chemistry*; Wiley-VHC: New York, 2008. (c) Lehn, J.-M. *Supramolecular Chemistry*; Wiley-VCH: New York, 1995.
(17) (a) Yang, H. B.; Ghosh, K.; Zhao, Y.; Northrop, B. H.; Lyndon, M. M.; Muddiman, D. C.; White, H. S.; Stang, P. J. *J. Am. Chem. Soc.* **2008**, *130*, 839−841. (b) Northrop, B. H.; Yang, H. B.; Stang, P. J. *Chem. Commun.* **2008**, *45*, 5896−5908. (c) You, C. C.; Würthner, F. *J. Am. Chem. Soc.* **2003**, *125*, 9716−9725. (d) Würthner, F.; You, C. C.; Saha-Möller, C. R. *Chem. Soc. Rev.* **2004**, *33*, 133−146.
(18) (a) Croue, V.; Goeb, S.; Salle, M. *Chem. Commun.* **2015**, *51*, 7275−7289. (b) Dinolfo, P. H.; Coropceanu, V.; Bredas, J.-L.; Hupp, J. T. *J. Am. Chem. Soc.* **2006**, *128*, 12592−12593. (c) Mahata, K.; Frischmann, P. D.; Würthner, F. *J. Am. Chem. Soc.* **2013**, *135*, 15656−15661. (d) Ghosh, K.; Hu, J. M.; White, H. S.; Stang, P. J. *J. Am. Chem. Soc.* **2009**, *131*, 6695−6697. (e) Bivaud, S.; Balandier, J.-Y.; Chas, M.; Allain, M.; Goeb, S.; Salle, M. *J. Am. Chem. Soc.* **2012**, *134*, 11968−11970. (f) Lewis, J. E. M.; Elliott, A. B. S.; McAdam, C. J.; Gordon, C. J.; Crowley, J. D. *Chem. Sci.* **2014**, *5*, 1833−1843.
(19) (a) Kaifer, A.; Gomez-Kaifer, M. *Supramolecular Electrochemistry*; Wiley-VCH: Weinheim, 1999. (b) Boulas, P. L.; Gomez-Kaifer, M.; Echegoyen, L. *Angew. Chem., Int. Ed.* **1998**, *37*, 216−247. (c) Nijhuis, C. A.; Ravoo, B. J.; Huskens, J.; Reinhoudt, D. N. *Coord. Chem. Rev.* **2007**, *251*, 1761−1780.
(20) (a) Ayme, J.-F.; Beves, J. E.; Campbell, C. J.; Leigh, D. A. *Chem. Soc. Rev.* **2013**, *42*, 1700. (b) Forgan, R. S.; Sauvage, J.-P.; Stoddart, J. F. *Chem. Rev.* **2011**, *111*, 5434. (c) Engelhard, D. M.; Freye, S.; Grohe, K.; John, M.; Clever, G. H. *Angew. Chem., Int. Ed.* **2012**, *51*, 4747.
(21) (a) Ward, M. D. *Chem. Soc. Rev.* **1997**, *26*, 365−375. (b) Wenger, O. S. *Coord. Chem. Rev.* **2015**, *282*−*283*, 150−158. (c) Natali, M.; Campagna, S.; Scandola, F. *Chem. Soc. Rev.* **2014**, *43*, 4005−15. (d) Guldi, D. M.; Imahori, H. *J. Porphyrins Phthalocyanines* **2004**, *8*, 976−983.
(22) Flynn, D. C.; Ramakrishna, G.; Yang, H.-B.; Northrop, B. H.; Stang, P. J.; Goodson, T. *J. Am. Chem. Soc.* **2010**, *132*, 1348−1358.
(23) Frasconi, M.; Kikuchi, T.; Cao, D.; Wu, Y.; Liu, W.-G.; Dyar, S. M.; Barin, G.; Sarjeant, A. A.; Stern, C. L.; Carmieli, R.; Wang, C.; Wasielewski, M. R.; Goddard, W. A.; Stoddart, J. F. *J. Am. Chem. Soc.* **2014**, *136*, 11011−11026.
(24) Barnes, J. C.; Frasconi, M.; Young, R. M.; Khdary, N. H.; Liu, W.-G.; Dyar, S. M.; McGonigal, P. R.; Gibbs-Hall, I. C.; Diercks, C. S.; Sarjeant, A. A.; Stern, C. L.; Goddard, W. A.; Wasielewski, M. R.; Stoddart, J. F. *J. Am. Chem. Soc.* **2014**, *136*, 10569−10572.
(25) Dirksen, A.; Kleverlaan, C. J.; Reek, J. N. H.; De Cola, L. *J. Phys. Chem. A* **2005**, *109*, 5248−5256.
(26) Schenning, A. P. H. J.; von Herrikhuyzen, J.; Jonkheijm, P.; Chen, Z.; Würthner, F.; Meijer, E. W. *J. Am. Chem. Soc.* **2002**, *124*, 10252−10253.
(27) Kawashima, Y.; Ohkubo, K.; Fukuzumi, S. *Chem. - Asian J.* **2015**, *10*, 44−54.
(28) (a) Park, J. S.; Karnas, E.; Ohkubo, K.; Chen, P.; Kadish, K. M.; Fukuzumi, S.; Bielawski, C. W.; Hudnall, T. W.; Lynch, V. M.; Sessler, J. L. *Science* **2010**, *329*, 1324−1327. (b) Fukuzumi, S.; Ohkubo, K.; D'Souza, F.; Sessler, J. L. *Chem. Commun.* **2012**, *48*, 9801−9815.
(29) Furutani, Y.; Kandori, H.; Kawano, M.; Nakabayashi, K.; Yoshizawa, M.; Fujita, M. *J. Am. Chem. Soc.* **2009**, *131*, 4764−4768.
(30) Porel, M.; Chuang, C.-H.; Burda, C.; Ramamurthy, V. *J. Am. Chem. Soc.* **2012**, *134*, 14718−14721.
(31) Oliva, A. I.; Ventura, B.; Würthner, F.; Camara-Campos, A.; Hunter, C. A.; Ballester, P.; Flamigni, L. *Dalton Trans.* **2009**, 4023−4037.
(32) Reviews: (a) Leininger, S.; Olenyuk, B.; Stang, P. J. *Chem. Rev.* **2000**, *100*, 853. (b) Fujita, M.; Umemoto, K.; Yoshizawa, M.; Fujita, N.; Kusukawa, T.; Biradha, K. *Chem. Commun.* **2001**, 509. (c) Seidel, S. R.; Stang, P. J. *Acc. Chem. Res.* **2002**, *35*, 972. (d) Pluth, M. D.; Raymond, K. N. *Chem. Soc. Rev.* **2007**, *36*, 161. (e) Dalgarno, S. J.; Power, P.; Atwood, J. L. *Coord. Chem. Rev.* **2008**, *252*, 825. (f) Tranchemontagne, D.; Ni, Z.; O'Keeffe, M.; Yaghi, O. *Angew. Chem., Int. Ed.* **2008**, *47*, 5136. (g) Chakrabarty, R.; Mukherjee, P. S.; Stang, P. J. *Chem. Rev.* **2011**, *111*, 6810. (h) Smulders, M. M. J.; Riddell, I. A.; Browne, C.; Nitschke, J. R. *Chem. Soc. Rev.* **2013**, *42*, 1728. (i) Custelcean, R. *Chem. Soc. Rev.* **2014**, *43*, 1813.
(33) Frank, M.; Hey, J.; Balcioglu, I.; Chen, Y.-S.; Stalke, D.; Suenobu, T.; Fukuzumi, S.; Frauendorf, H.; Clever, G. H. *Angew. Chem., Int. Ed.* **2013**, *52*, 10102−10106.
(34) (a) Dwivedi, P. C.; Gurudath Rao, K.; Bhat, S. N.; Rao, C. N. R. *Spectrochim. Acta* **1975**, *31A*, 129−135. (b) McCafferty, D. G.; Bishop, B. M.; Wall, C. G.; Hughes, S. G.; Mecklenberg, S. M.; Meyer, T. J.; Erickson, B. W. *Tetrahedron* **1995**, *51*, 1093−1106. (c) Mecklenburg, S. L.; McCafferty, D. G.; Schoonover, J. R.; Peek, B. M.; Erickson, B. W.; Meyer, T. J. *Inorg. Chem.* **1994**, *33*, 2974−2983. (d) Striplin, D. R.; Reece, S. Y.; McCafferty, D. G.; Wall, C. G.; Friesen, D. A.; Erickson, B. W.; Meyer, T. J. *J. Am. Chem. Soc.* **2004**, *126*, 5282−5291. (e) Myers, C. P.; Williams, M. E. *Coord. Chem. Rev.* **2010**, *254*, 2416−2428. (f) Zhang, W.-W.; Mao, W.-L.; Hu, Y.-X.; Tian, Z.-Q.; Wang, Z.-L.; Meng, Q.-J. *J. Phys. Chem. A* **2009**, *113*, 9997−10004. (g) Bay, S.; Villnow, T.; Ryseck, G.; Rai-Constapel, V.; Gilch, P.; Müller, T. J. J. *ChemPlusChem* **2013**, *78*, 137−141.
(35) (a) Fukuda, M.; Sekiya, R.; Kuroda, R. *Angew. Chem., Int. Ed.* **2008**, *47*, 706−710. (b) Freye, S.; Hey, J.; Torras-Galan, A.; Stalke, D.; Herbst-Irmer, R.; John, M.; Clever, G. H. *Angew. Chem., Int. Ed.* **2012**, *51*, 2191−2194. (c) Freye, S.; Engelhard, D. M.; John, M.; Clever, G. H. *Chem. - Eur. J.* **2013**, *19*, 2114−2121. (d) Freye, S.; Michel, R.; Stalke, D.; Pawliczek, M.; Frauendorf, H.; Clever, G. H. *J. Am. Chem. Soc.* **2013**, *135*, 8476−8479. (e) Han, M.; Engelhard, D. M.; Clever, G. H. *Chem. Soc. Rev.* **2014**, *43*, 1848−1860. (f) Zhu, R.; Lübben, J.; Dittrich, B.; Clever, G. H. *Angew. Chem., Int. Ed.* **2015**, *54*, 2796−2800. (g) Löffler, S.; Lübben, J.; Krause, L.; Stalke, D.; Dittrich, B.; Clever, G. H. *J. Am. Chem. Soc.* **2015**, *137*, 1060−1063.

DOI: 10.1021/jacs.6b04609
J. Am. Chem. Soc. 2016, 138, 8279−8287

(36) Frank, M.; Krause, L.; Herbst-Irmer, R.; Stalke, D.; Clever, G. H. *Dalton Trans.* **2014**, *43*, 4587−4592.
(37) Knibbe, H.; Rehm, D.; Weller, A. *Ber. Bunsen-Ges. Phys. Chem.* **1968**, *72*, 257−262.
(38) The oxidized/reduced species with the formally highest/lowest possible charge are mentioned in the discussion of the electrochemical studies for the sake of simplicity, while the formation of partially oxidized/reduced species cannot be ruled out under the experimental conditions. This does not affect the interpretations since only difference spectra are compared.
(39) Yang, J. H.; Dass, A.; Rawashdeh, A.-M. M.; Sotiriou-Leventis, C.; Panzner, M. J.; Tyson, D. S.; Kinder, J. D.; Leventis, N. *Chem. Mater.* **2004**, *16*, 3457−3468.
(40) Lauer, A.; Dobryakov, A. L.; Kovalenko, S. A.; Fidder, H.; Heyne, K. *Phys. Chem. Chem. Phys.* **2011**, *13*, 8723−8732.
(41) Shirdel, J.; Penzkofer, A.; Prochazka, R.; Shen, Z.; Daub, J. *Chem. Phys.* **2007**, *336*, 1−13.
(42) Alkaitis, S. A.; Beck, G.; Grätzel, M. *J. Am. Chem. Soc.* **1975**, *97*, 5723−5729.

DOI: 10.1021/jacs.6b04609
J. Am. Chem. Soc. 2016, 138, 8279−8287